INTERNATIONAL ATOMIC ENERGY AGENCY
UNITED NATIONS EDUCATIONAL, SCIENTIFIC AND CULTURAL ORGANIZATION

INTERNATIONAL CENTRE FOR THEORETICAL PHYSICS
34100 TRIESTE (ITALY) - P.O.B. 586 - MIRAMARE - STRADA COSTIERA 11 - TELEPHONES: 224281/2/3/4/5 6
CABLE: CENTRATOM - TELEX 460392-1

SMR/100 - 41

WINTER COLLEGE ON LASERS, ATOMIC AND MOLECULAR PHYSICS

(24 January - 25 March 1983)

Laser Beam Transformation

O. SVELTO

Centro di Elettronica Quantistica
e Strumentazione Elettronica
Istituto di Fisica del Politecnico
Piazza Leonardo da Vinci, 32
20133 Milano
Italy

8

Laser Beam Transformation

8.1 INTRODUCTION

Before it is put to use, a laser beam is generally transformed in some way. The most common type of transformation is that which occurs when the beam is made to propagate in free space or through a suitable optical system. Since this produces a change in the spatial distribution of the beam (e.g., the beam may be focused or expanded), we shall refer to this as a *spatial transformation* of the laser beam. A second type of transformation, also rather frequently encountered, is that which occurs when the beam is passed through an amplifier or chain of amplifiers. Since the main effect here is to alter the beam amplitude, we shall refer to this as *amplitude transformation*. A third, less trivial, case occurs when the wavelength of the beam is changed as a result of propagating through a suitable nonlinear optical material (*wavelength transformation*). Finally, the temporal behavior of the laser beam can be modified (e.g., the time variation of the output from a pulsed laser may be changed) by a suitable electro-optical or nonlinear optical element. This fourth and last case will be called *time transformation*. It should be noted that these four types of beam transformation are often interrelated. For instance, amplitude and wavelength transformation often result in spatial and time transformations occurring as well.

In this chapter the cases of spatial, amplitude, and wavelength transformation will be briefly considered. In the case of wavelength transformation, of the various nonlinear optical effects which can be used[1] to achieve this, only the so-called parametric effects will be considered here. These in fact provide some of the most useful techniques so far developed for producing new sources of coherent light. Time transformations will not

[illegible] We also [illegible]ve out some amplitude and time transformations arising from the nonlinear phenomena of self-focusing and self-phase-modulation,[2] although it should be noted that they can play a very important role in limiting the performance of laser amplifiers.

8.2 TRANSFORMATION IN SPACE: GAUSSIAN BEAM PROPAGATION

In this section we will limit ourselves to considering the propagation of a lowest-order Gaussian beam (TEM_{00} mode). The important topics of propagation of coherent beams having non-Gaussian transverse distributions (for which the Kirchhoff integral or equation (8.10) can still be used) and propagation of partially coherent beams[3] will not be considered.

The case of free-space propagation of a TEM_{00} Gaussian beam has already been considered in Chapter 7 (see Section 7.4). For convenience we repeat here the expressions for beam spot size w and radius of curvature R of the equiphase surfaces, viz.,

$$w^2 = w_0^2\left[1 + \left(\frac{\lambda z}{\pi w_0^2}\right)^2\right] \tag{8.1a}$$

$$R = z\left[1 + \left(\frac{\pi w_0^2}{\lambda z}\right)^2\right] \tag{8.1b}$$

where w_0 is the spot size at the beam waist and the z coordinate is measured along the propagation direction with its origin at the waist.† Figure 8.1 shows the behavior of the beam spot size and equiphase surfaces with distance z. We re-emphasize that the propagation properties of this beam depend only on the wavelength and the value w_0 of the spot size at the beam waist. We also recall that this can be understood by noting that, once w_0 is known, both the amplitude and phase are known at the waist (the wavefront is plane at the waist). Since the field distribution is thus known over the entire plane $z = 0$, diffraction theory [e.g., the Kirchhoff integral (4.10)] can be used to calculate the field amplitude at any given point in space. We shall not carry out such a calculation here and we limit ourselves to noting that equation (8.1a) shows that the square of the beam spot size at a distance z from the waist is given by the sum of the squares of the spot

†We recall that the sign convention for radius of curvature is that $R(z)$ is taken as positive when the center of curvature is to the left of the wavefront.

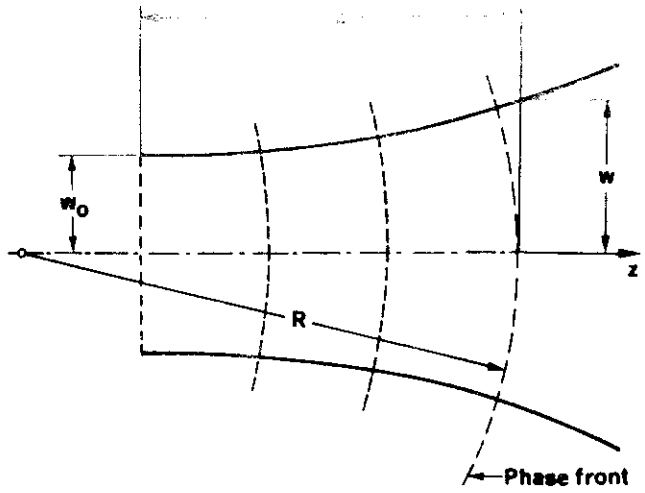

FIG. 8.1. Propagation of a Gaussian beam.

size at the waist, w_0^2, and the contribution $[(\lambda/\pi w_0)z]^2$ arising from diffraction. At the end of this section, as an exercise, equations (8.1) will be derived directly from Maxwell's equations rather than using the Kirchhoff integral.

We now turn our attention to the propagation of a TEM_{00} Gaussian beam through a lens system. Figure 8.2 depicts the behavior of the beam as a result of passing through a lens of focal length f. We begin by noting that, just before the lens, the spot size w_1 and radius of curvature R_1 of the beam can, according to (8.1), be written as

$$w_1^2 = w_{01}^2\left[1 + \left(\frac{\lambda L_1}{\pi w_{01}^2}\right)^2\right] \tag{8.2a}$$

$$R_1 = L_1\left[1 + \left(\frac{\pi w_{01}^2}{\lambda L_1}\right)^2\right] \tag{8.2b}$$

We also note that, for a thin lens, the amplitude distribution must remain unchanged upon passing through the lens, i.e., there cannot be a discontinuous change of spot size. Thus we can write

$$w_2 = w_1 \tag{8.3a}$$

for the beam spot size after the lens. To calculate the corresponding wavefront curvature we first consider the case of propagation of a spherical

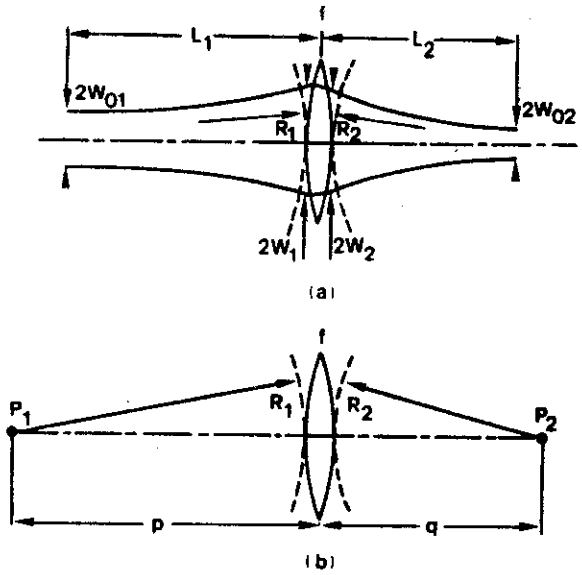

FIG. 8.2. (a) Propagation of a Gaussian beam through a lens; (b) propagation of a spherical wave through a lens.

wave through the same lens (Fig. 8.2*b*). Here a spherical wave originating from a source point P_1 is focused by the lens to the image point P_2. From geometrical optics there follows the well-known result that $p^{-1} + q^{-1} = f^{-1}$. Since the radii of curvature R_1 and R_2 of the two spherical waves just before and after the lens are equal to p and $-q$ respectively† we can also write

$$\frac{1}{R_1} - \frac{1}{R_2} = \frac{1}{f} \tag{8.3b}$$

A spherical lens can then be seen to transform the radius of curvature R_1 of an incoming wave to a radius R_2 of the outgoing wave according to (8.3*b*). Similarly, the radius of curvature R_2 of the outgoing Gaussian beam of Fig. 8.2a will also be given by (8.3*b*), and so we now have both the amplitude [through (8.3*a*)] and phase [through (8.3*b*)] distribution of the outgoing wave. This wave therefore has a Gaussian amplitude distribution and spherical wavefront, i.e., a Gaussian beam remains a Gaussian beam after passing through a (thin) lens system. This result applies also to a thick lens

†Note the application of the sign convention referred to earlier.

system, as can be seen by considering a thick lens as a sequence of thin lenses. Once the spot size and radius of curvature of the outgoing wave are known just after the lens, we can calculate the corresponding values at any points in space. For instance, the spot size w_{02} at the new beam waist and the distance L_2 of this waist from the lens can be obtained by using equations (8.1) in reverse. After some straightforward manipulation we arrive at the following two equations:

$$L_1 = f \pm \left(\frac{w_{01}}{w_{02}}\right)(f^2 - f_0^2)^{1/2} \tag{8.4a}$$

$$L_2 = f \pm \left(\frac{w_{02}}{w_{01}}\right)(f^2 - f_0^2)^{1/2} \tag{8.4b}$$

from which both w_{02} and L_2 can be obtained. The quantity f_0 in equations (8.4) is given by

$$f_0 = \pi w_{01} w_{02}/\lambda \tag{8.5}$$

and either the two plus or the two minus signs can be chosen. These equations prove very useful for solving a variety of problems which arise in Gaussian beam propagation (see Problems 8.2 and 8.3). We limit ourselves to pointing out here that, when the first waist is coincident with the first focal plane ($L_1 = f$), the second waist also coincides with the second focal plane of the lens ($L_2 = f$). We also note that, in general, the planes of the two waists are not conjugated in accordance with the geometrical optics result (i.e., $L_1^{-1} + L_2^{-1} \neq f^{-1}$).

Before ending this section we show, as an exercise, how (8.1) can be derived through Maxwell's equations rather than using the Kirchhoff integral. In the scalar case, Maxwell's equations lead to the wave equation†

$$\nabla^2 E - \frac{1}{c^2}\frac{\partial^2 E}{\partial t^2} = 0 \tag{8.6}$$

For a monochromatic wave we write $E(x, y, z, t) = E(x, y, z)\exp(i\omega t)$, and equation (8.6) gives (Helmholtz equation)

$$\nabla^2 E(x, y, z) + k^2 E(x, y, z) = 0 \tag{8.7}$$

with $k = \omega/c$. For a radially symmetric beam, expressing (8.7) in cylindrical coordinates gives

$$\left(\frac{\partial^2}{\partial r^2} + \frac{1}{r}\frac{\partial}{\partial r} + \frac{\partial^2}{\partial z^2}\right)E + k^2 E = 0 \tag{8.8}$$

†It has been pointed out[15] that some care is needed to derive this equation in a rigorous fashion.

We now look for a solution of the form

$$E(r,z) = U(r,z)\exp(-ikz) \tag{8.9}$$

in which $U(r,z)$, as a function of z, is assumed to be slowly varying on the scale of a wavelength ($\lambda = 2\pi/k$). Substituting (8.9) into (8.8), and using this slowly varying amplitude approximation (i.e., putting $\partial^2 U/\partial^2 z \ll k\partial U/\partial z$) gives

$$\left(\frac{\partial^2}{\partial r^2} + \frac{1}{r}\frac{\partial}{\partial r}\right)U - 2ik\frac{\partial U}{\partial z} = 0 \tag{8.10}$$

This is the fundamental equation we require (known as the quasi-optical equation) and is widely used in diffraction theory. It has to be solved with the appropriate boundary conditions.

To solve (8.10) in our case, we set the boundary condition (see Fig. 8.1)

$$U(r,0) = \exp(-r/w_0)^2 \tag{8.11}$$

Accordingly, for $z > 0$, we look for a solution of the general Gaussian form

$$U(r,z) = \exp(\alpha - \beta r^2) \tag{8.12}$$

where both α and β are taken to be complex functions of z. Before proceeding it is appropriate to point out the physical significance of both α and β. The real part of α gives the change in amplitude on the beam axis (where $r = 0$) due to beam propagation. The imaginary part of α gives a phase shift which is additional to the plane wave phase shift kz already included in (8.9). The real part, β_r, of β is obviously related to the beam spot size w by the equation

$$\beta_r = 1/w^2 \tag{8.13}$$

To understand the meaning of the imaginary part, β_i, of β, consider a uniform spherical wave emitted from a point source P located at $z = 0$ (Fig. 8.3). The field $U(P_2)$ of this wave at point P_2 lying on a plane which is perpendicular to the z axis and which is placed at a distance R from point

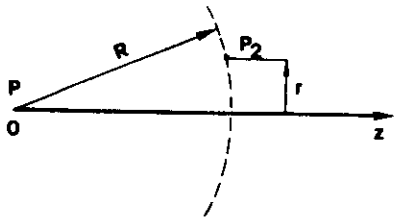

FIG. 8.3. Phase value at point $P_2(z = R)$ for a spherical wave originating from point P $(z = 0)$.

P is

$$U(P_2) \propto \frac{\exp\left[-ik(r^2+R^2)^{1/2}\right]}{\left[r^2+R^2\right]^{1/2}}$$

$$\simeq \frac{\exp(-ikR)}{R}\exp\left[-(ikr^2/2R)\right] \qquad \text{for } r \ll R \tag{8.14}$$

Note that R is also the radius of curvature of the spherical wave at the plane considered (dashed arc in Fig. 8.3). We thus recognize that a phase term of the form $kr^2/2R$ must represent a spherical wavefront of radius R. The comparison of the phase term $i\beta_i r^2$ in (8.12) with the phase term $ikr^2/2R$ in (8.14) then shows that β_i is related to the radius of curvature of the wavefront by

$$\beta_i = k/2R \tag{8.15}$$

We are now ready to substitute (8.12) into the wave equation (8.10) and use the boundary condition (8.11). The substitution gives

$$r^2\left(ik\frac{d\beta}{dz} + 2\beta^2\right) - \left(ik\frac{d\alpha}{dz} + 2\beta\right) = 0 \tag{8.16}$$

Since this expression must be zero for any r, each of the two terms in brackets must be zero, i.e.,

$$ik\frac{d\beta}{dz} + 2\beta^2 = 0 \tag{8.17a}$$

$$ik\frac{d\alpha}{dz} + 2\beta = 0 \tag{8.17b}$$

The solution of (8.17a) with the boundary condition (8.11) gives

$$\beta = \frac{ik}{2\left(z + i\dfrac{\pi w_0^2}{\lambda}\right)} \tag{8.18}$$

With the help of (8.18) and again using the boundary condition (8.11), we obtain from (8.17b)

$$\alpha = -\ln\left(1 - \frac{iz\lambda}{\pi w_0^2}\right) \tag{8.19}$$

Calculating the real and imaginary parts of β from (8.18) and using the relations (8.13) and (8.15) then yields equations (8.1a) and (8.1b) respectively. Equation (8.19), with the help of (8.1a), can be expressed in the form

$$\exp\alpha = \frac{w_0}{w}\exp i\phi \tag{8.20}$$

represents the additional phase shift to be added to the usual plane wave phase shift. From (8.9), (8.12), (8.13), (8.15), and (8.20) we finally get the complete expression for the field amplitude as [compare with (4.33)]

$$E(r,z) = \frac{w_0}{w} \exp\left[-i(kz - \phi) - r^2\left(\frac{1}{w^2} + \frac{ik}{2R}\right)\right] \tag{8.22}$$

Note that the field amplitude at $r = 0$ (i.e., on the beam axis) scales as w_0/w. Note also that, strictly speaking, the equiphase surfaces are really paraboloids rather than spheres. The equiphase surface which cuts the z axis at $z = z_0$ must have a phase which is at all points the same as the phase given by (8.22) for the particular point $r = 0$ and $z = z_0$, i.e., $\phi(z) - k[z + (r^2/2R)] = \phi(z_0) - kz_0$. Neglecting the small term ϕ, we see that the previous equation corresponds to a paraboloid cutting the z axis at $z = z_0$. Thus the radius of curvature R is in fact the radius of curvature of this paraboloid on the beam axis (i.e., for $r = 0$).

8.3 TRANSFORMATION IN AMPLITUDE: LASER AMPLIFICATION[4–6]

In this section we consider the rate-equation treatment of a laser amplifier. We assume that a plane wave of uniform intensity I enters (at $z = 0$) a laser amplifier extending for a length l along the z direction. We limit our considerations to a situation where the incident radiation is in the form of a pulse of duration τ_p such that $\tau_1 \ll \tau_p \ll (\tau, W_p^{-1})$, where τ_1 and τ are respectively the lifetime of the lower and upper levels of the amplifier medium and where W_p is the amplifier pump rate. This is perhaps the most relevant set of conditions for laser amplification and applies, for instance, when a Q-switched laser pulse from a Nd:YAG laser needs to be amplified. The case of cw amplification (steady-state amplification) is therefore not considered here and we refer the reader elsewhere for a discussion of this topic.[5–6]

Given these assumptions, the population of the lower level of the amplifier can be set equal to zero, and pumping and decay of the upper level of the amplifier during the passage of the pulse can be neglected. The rate of change of population inversion $N(t,z)$ at a point z within the amplifier can then be written with the help of (2.60) [in which we put

$$\frac{\partial N}{\partial t} = -WN = -\frac{I}{\Gamma_s} \tag{8.23}$$

where

$$\Gamma_s = \frac{h\nu}{\sigma} \tag{8.24}$$

is a parameter which depends only on the laser material. Note that a partial derivative is required in (8.23) since we expect N to be a function of both z and t, i.e., $N = N(t,z)$, on account of the fact that $I = I(t,z)$. Next we derive a differential equation describing the temporal and spatial variation of intensity I. To do this we first consider the rate of change of energy density ρ of the light wave (where $\rho = I/c$, hence $\partial I/c\partial t = \partial\rho/\partial t$). By considering the net rate of change of photon energy within a small volume of the amplifier (see Fig. 8.4) we can write

$$\frac{1}{c}\frac{\partial I}{\partial t} = \frac{\partial \rho}{\partial t} = \left(\frac{\partial \rho}{\partial t}\right)_1 + \left(\frac{\partial \rho}{\partial t}\right)_2 + \left(\frac{\partial \rho}{\partial t}\right)_3 \tag{8.25}$$

where $(\partial\rho/\partial t)_1$ accounts for stimulated emission and absorption in the amplifier, $(\partial\rho/\partial t)_2$ for the amplifier loss (e.g., scattering losses), and $(\partial\rho/\partial t)_3$ for the net photon flux which flows into the volume. With the help of (2.60) [$F = I/h\nu$] we obtain

$$\left(\frac{\partial \rho}{\partial t}\right)_1 = WNh\nu = \sigma NI \tag{8.26}$$

and from (2.60) and (2.64) we obtain

$$\left(\frac{\partial \rho}{\partial t}\right)_2 = -W_a N_a h\nu = -\alpha I \tag{8.27}$$

where N_a is the density, W_a the absorption rate, and α the absorption coefficient of the loss centers. To calculate $(\partial\rho/\partial t)_3$, we refer to Fig. 8.4 where an elemental volume of the amplifier material of length dz and unit cross section is indicated by the shaded region. The quantity $(\partial\rho/\partial t)_3\,dz$ is the rate of change of photon energy in this volume due to the difference

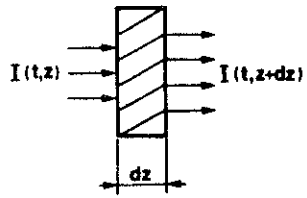

FIG. 8.4. Rate of change of the photon energy contained in an elemental volume dz (unit cross section) of the laser amplifier

between the input and output intensity, i.e.,

$$\left(\frac{\partial I}{\partial t}\right)_1 dz = I(t,z) - I(t,z+dz) = -\frac{\partial I}{\partial z}\,dz \tag{8.28}$$

From (8.25) to (8.28) we then obtain the equation

$$\frac{1}{c}\frac{\partial I}{\partial t} + \frac{\partial I}{\partial z} = \sigma N I - \alpha I \tag{8.29}$$

which together with (8.23) completely describes the amplification behavior. Note that (8.29) has the usual form of a time-dependent transport equation. Note also that, in the steady state and for $\alpha = 0$, it reduces to (1.7).

Equations (8.23) and (8.29) must now be solved with the appropriate boundary and initial conditions. As the initial condition we take $N(0,z) = N_0 = \text{const}$, where N_0 is established by pumping of the amplifier before the arrival of the laser pulse. The boundary condition is obviously established by the intensity $I_0(t)$ of the light pulse which is injected into the amplifier, i.e., $I(t,0) = I_0(t)$. For negligible amplifier losses (i.e., neglecting the term $-\alpha I$), the solution to (8.29) can be written as

$$I(z,\tau) = I_0(\tau)\left\{1 - \left[1 - \exp(-g_0 z)\right]\exp\left[-\int_{-\infty}^{\tau} I_0(\tau')\,d\tau'/\Gamma_s\right]\right\}^{-1} \tag{8.30}$$

where $\tau = t - (z/c)$ and where $g_0 = \sigma N_0$ is the unsaturated gain coefficient of the amplifier. From (8.29), one can also readily obtain an equation for the total laser energy fluence

$$\Gamma(z) = \int_{-\infty}^{+\infty} I(z,t)\,dt \tag{8.31}$$

Integrating both sides of (8.29) with respect to time, from $t = -\infty$ to $t = +\infty$, and using (8.23), we get

$$\frac{d\Gamma}{dz} = g_0\Gamma_s\left[1 - \exp(-\Gamma/\Gamma_s)\right] - \alpha\Gamma \tag{8.32}$$

Again neglecting amplifier losses, (8.32) gives

$$\Gamma(l) = \Gamma_s \ln\left\{1 + \left[\exp\left(\frac{\Gamma_{in}}{\Gamma_s}\right) - 1\right]G_0\right\} \tag{8.33}$$

where $G_0 = \exp g_0 l$ is the unsaturated amplifier gain and Γ_{in} the energy fluence of the input beam. As a representative example the ratio Γ/Γ_s is plotted in Fig. 8.5 versus Γ_{in}/Γ_s for $G_0 = 3$. Note that, for $\Gamma_{in} \ll \Gamma_s$, (8.33) can be approximated as

$$\Gamma(l) = G_0\Gamma_{in} \tag{8.34}$$

and the output fluence increases linearly with the input fluence (linear amplification regime). Equation (8.34) is also plotted in Fig. 8.5 as a dashed straight line starting from the origin. At higher input fluences, however, Γ increases with Γ_{in} at a lower rate than that predicted by (8.34) (see Fig. 8.5), i.e., amplifier saturation occurs. Thus Γ_s may be called the saturation energy fluence of the amplifier. For $\Gamma_{in} \gg \Gamma_s$ (saturation regime) we get

$$\Gamma(l) = \Gamma_{in} + \Gamma_s g_0 l \tag{8.35}$$

Equation (8.35) has also been plotted in Fig. 8.5 as a dashed straight line. Note that (8.35) shows that, for high input fluences, the output fluence is linearly dependent on the length l of the amplifier. Since $\Gamma_s g_0 l = N_0 l h\nu$, we see that every excited atom undergoes stimulated emission and thus contributes its energy to the beam. Such a condition obviously represents the most efficient conversion of stored energy to beam energy, and for this reason amplifier designs operating in the saturation regime are used wherever practical.

If amplifier losses are present, the above picture is somewhat modified. In particular the output fluence $\Gamma(l)$ does not continue to increase with input fluence (as in Fig. 8.5) but reaches a maximum and then decreases. This can be understood by noting that the output as a function of amplifier length tends to grow linearly due to amplification [at least for high input fluences, see (8.35)] and to decrease exponentially due to loss [on account of the term $-\alpha\Gamma$ in (8.32)]. The competition of these two terms then gives a

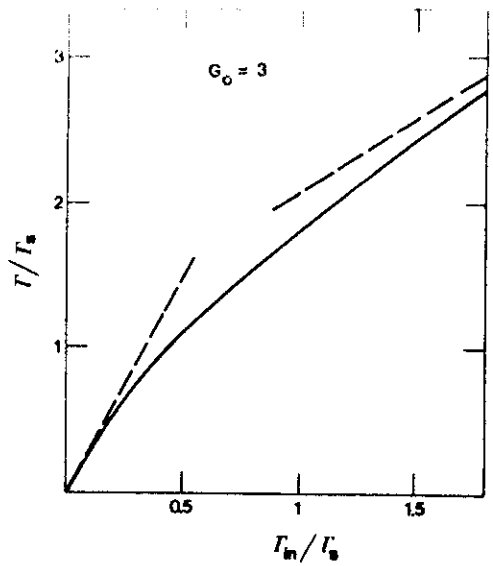

FIG. 8.5. Output laser energy fluence Γ versus input fluence Γ_{in} for a laser amplifier with a small signal gain $G_0 = 3$. The energy fluence is normalized to the laser saturation fluence $\Gamma_s = h\nu/\sigma$.

maximum for the output fluence Γ. For $\alpha \ll g_0$ this maximum value of the output fluence is

$$\Gamma \simeq g_0 \Gamma_s / \alpha \tag{8.36}$$

Since, however, amplifier losses are typically quite small, other phenomena usually limit the maximum energy fluence that can be extracted from an amplifier. In fact, the limit is usually set by the amplifier damage fluence Γ_d (of the order of 10 J/cm^2 in some practical cases). From (8.35) we then get

$$\Gamma \simeq \Gamma_s g_0 l < \Gamma_d \tag{8.37}$$

On the other hand, the unsaturated gain $G_0 = \exp(g_0 l)$ must not be made too high, otherwise two undesirable effects can occur in the amplifier: (i) parasitic oscillations, (ii) amplified spontaneous emission (ASE). Parasitic oscillation occurs when the amplifier starts lasing by virtue of some internal feedback which will always be present to some degree (e.g., due to the amplifier end faces). The phenomenon of ASE has already been discussed in Section 2.3.4. Both these phenomena tend to depopulate the available inversion and hence decrease the laser gain. To minimize parasitic oscillations one should avoid elongated amplifiers and in fact ideally use amplifiers with approximately equal dimensions in all directions. Even in this case, however, parasitic oscillations set an upper limit $(g_0 l)_{\max}$ to the available gain coefficient g_0 times the amplifier length, l, i.e.,

$$g_0 l < (g_0 l)_{\max} \tag{8.38}$$

and $(g_0 l)_{\max}$ may be of the order of 3 to 5 in practical cases. The threshold for ASE has already been given in Section 2.3.4 [equation (2.91*b*)]. For an amplifier in the form of a cube (i.e., for $\Omega \simeq 1$) we get $G \simeq 5.1$ [i.e., $g_0 l \simeq 1.6$] which is of the same order as that established by parasitic oscillations. For smaller values of solid angle Ω (as is more common), the value of G for the onset of ASE increases [equation (2.91*b*)]. Hence parasitic oscillations, rather than ASE, usually determine the maximum gain that can be achieved. Taking into account both the limit due to damage, (8.37), and the limit due to parasitic oscillations, (8.38), we can readily obtain an expression for the maximum energy E_m which can be extracted from an amplifier as

$$E_m = \Gamma_d l_m^2 = \Gamma_d (g_0 l)_m^2 / g_0^2 \tag{8.39}$$

where l_m is the maximum amplifier dimension (for a cubic amplifier) implied by (8.38). Equation (8.39) shows that E_m is increased by decreasing the amplifier gain coefficient g_0. A limit to this reduction of g_0 would ultimately be established by the amplifier losses α. Taking, as an example, $g_0 \simeq 10^{-2}$ cm^{-1} and $\Gamma_d = 10$ J/cm^2, we get from (8.39) $E_m \simeq 1$ MJ. This, however, would require an amplifier dimension of the order of $l_m \simeq (g_0 l)_m / g_0 \simeq 4$ m, which is somewhat impracticable.

So far we have concerned ourselves mostly with the change of a laser pulse energy as it passes through an amplifier. In the saturation regime, however, important changes in both the temporal and spatial shape of the input beam also occur. The spatial distortions can be readily understood with the help of Fig. 8.5. For an input beam with a bell-shaped transverse intensity profile (e.g., a Gaussian beam), the beam center, as a result of saturation, will experience less gain than the periphery of the beam. Thus, the width of the beam's spatial profile is enlarged as the beam passes through the amplifier. The reason for temporal distortions can also be seen quite readily. Stimulated emission caused by the leading edge of the pulse implies that some of the stored energy has already been extracted from the amplifier by the time the trailing edge of the pulse arrives, which will therefore see a smaller population inversion and thus experience a reduced gain. As a result, less energy is added to the trailing edge than to the leading edge of the pulse, and this leads to considerable pulse reshaping. The output pulse shape can be calculated from (8.30), and it is found that the pulse may either get broader or narrower (or even remain unchanged) due to this phenomenon, the outcome depending upon the shape of the input pulse.[4]

To conclude this section we will briefly examine two further examples of laser amplification, involving conditions different from those considered above. In the first case the duration τ_p of the pulse to be amplified is assumed to be much shorter than the lifetime of the lower laser level.† This is, for instance, the situation in a ruby amplifier in which the lower laser level is coincident with the ground level. This is also the situation in a neodymium amplifier when $\tau_p < 1$ ns. In both previous cases the amplifier behaves like a three-level system, and it can be readily shown that the previous equations still apply provided Γ_s is now given by

$$\Gamma_s = h\nu / 2\sigma \tag{8.39a}$$

The second case we briefly consider is that of an amplifier in which both the upper and lower levels are made up of many sublevels which are strongly coupled. This applies, for instance, to CO_2 or HF amplifiers whose upper and lower (vibrational) states consist of many rotational levels (see, for example, Fig. 6.13). If the pulse duration is much longer than the time for relaxation between rotational levels, then the thermal equilibrium

†We will, however, assume $\tau_p \gg T_2$, where $T_2 = 1/\pi\Delta\nu_0$, this being a necessary condition for the validity of the rate-equation approximation (see Section 5.5).

population distribution will be maintained among these levels. The population N_j of a rotational level belonging to a given vibrational state can then be written as a fraction of the total population N of the vibrational state (see Section 2.7), where z (the partition function) can be calculated according to Boltzmann statistics. We further assume that: (i) The pulse duration τ_p is much shorter than the relaxation time of the lower laser level (so that the system effectively behaves like a three-level system). (ii) The wavelength of the incoming light pulse corresponds to just one rotational–vibrational line. In this case all the previous results will again apply provided we take[6]

$$\Gamma_s = h\nu/2\sigma z \tag{8.39b}$$

where σ is the stimulated emission cross section for the rotational–vibrational transition involved in the amplification process. A comparison of (8.39b) with (8.39a) then shows that we can define an effective cross section as $z\sigma$ [see also equations (2.142m) and (2.142n)]. When the pulse duration becomes comparable with the rotational relaxation time, the picture becomes much more involved, and calculations using the resulting equations generally require the use of computers.[6]

8.4 TRANSFORMATION IN FREQUENCY: SECOND-HARMONIC GENERATION AND PARAMETRIC OSCILLATION[7-9]

In classical linear optics one assumes that the induced dielectric polarization of a medium is linearly related to the applied electric field, i.e.,

$$\mathbf{P} = \varepsilon_0 \chi \mathbf{E} \tag{8.40}$$

where χ is the dielectric susceptibility. With the high electric fields involved in laser beams the above linear relation is no longer a good approximation and further terms in which $\mathbf{P}$ is related to higher-order powers of $\mathbf{E}$ must also be considered. This nonlinear response can lead to an exchange of energy between e.m. waves at different frequencies.

In this section we will consider some of the effects produced by a nonlinear polarization term which is proportional to the square of the electric field. The two effects that we will consider are: (i) Second-Harmonic Generation (SHG) in which a laser beam at frequency ω is partially converted, in the nonlinear material, to a coherent beam at frequency 2ω (as first shown by Franken *et al.*[10]); (ii) Optical Parameter Oscillation (OPO) in which a laser beam at frequency ω_3 causes the simultaneous generation, in the nonlinear material, of two coherent beams at frequency ω_1 and ω_2 such that $\omega_1 + \omega_2 = \omega_3$ (as first shown by Giordmaine and Miller[11]). With the high electric fields available in laser beams the conversion efficiency of both these processes can be very high (approaching 100% in SHG). These techniques are therefore currently being used to generate new coherent waves at different frequencies from that of the incoming wave.

8.4.1 Physical Picture

We will first introduce some ideas using the simplifying assumption that the induced nonlinear polarization P^{NL} is related to the electric field E of the e.m. wave by a scalar equation, i.e.,

$$P^{NL} = 2\varepsilon_0 dE^2 \tag{8.41}$$

where d is a coefficient whose dimension is the inverse of an electric field.† The physical origin of (8.41) is due to the nonlinear deformation of the outer, loosely bound, electrons of an atom or atomic system when subjected to high electric fields. This is analogous to a breakdown of Hooke's law for an extended spring, i.e., the restoring force is no longer linearly dependent on the displacement from equilibrium. A comparison of (8.41) and (8.40) shows that the nonlinear polarization term becomes comparable to the linear one for an electric field $E \simeq \chi/d$. Since $\chi \simeq 1$, we see that $(1/d)$ must be that field strength at which the linear and nonlinear terms become comparable, i.e., at which a sizable nonlinear deformation of the outer electrons will occur. Thus $1/d$ is expected to be of the order of the electric field which an electronic charge produces at a distance corresponding to a typical atomic dimension a, i.e., $(1/d) \simeq e/4\pi\varepsilon_0 a^2$ [thus $(1/d) \sim 10^{11}$ V/m for $a \simeq 1$ Å]. We note that, for symmetry reasons, d must be zero for a centrosymmetric material (such as for a centrosymmetric crystal and usually for liquids and gases). For symmetry reasons, in fact, if we reverse the sign of E, the sign of the total polarization $P_T = P + P^{NL}$ must also reverse. Since, however, $P^{NL} \propto E^2$, this can only occur if $d = 0$. From now on we will therefore confine ourselves to a consideration of noncentrosymmetric materials. We will see that the simple equation (8.41) is in this case able to account for both SHG and OPO.

8.4.1.1 Second-Harmonic Generation

We consider a monochromatic plane wave of frequency ω propagating in the z direction through a nonlinear crystal. For a plane wave of uniform

†We use $2\varepsilon_0 dE^2$ rather than dE^2 (as often used in other textbooks) to make d conform to increasingly accepted practice.

intensity we can write the following expression for the electric field $E_\omega(z,t)$ of the wave:

$$E_\omega(z,t) = \tfrac{1}{2}\left\{ E(z,\omega)\exp\left[i(\omega t - k_\omega z)\right] + \text{c.c.}\right\} \tag{8.42}$$

In the above expression c.c. means the complex conjugate of the other term appearing in the braces and

$$k_\omega = \frac{\omega}{c_\omega} = \frac{n_\omega}{c_0} \tag{8.43}$$

where c_ω is the light velocity in the crystal, n_ω is the refractive index at frequency ω, and c_0 is the velocity of light *in vacuo*. Substitution of (8.42) into (8.41) shows that P^{NL} contains a term† oscillating at frequency 2ω, namely

$$P^{\text{NL}}_{2\omega} = \frac{\varepsilon_0 d}{2}\left\{ E^2(z,\omega)\exp\left[i(2\omega t - 2k_\omega z)\right] + \text{c.c.}\right\} \tag{8.44}$$

Equation (8.44) describes a polarization oscillating at frequency 2ω and whose spatial variation is in the form of a wave. This polarization wave will radiate at frequency 2ω. Thus it generates an e.m. wave at the second harmonic frequency 2ω [the analytical treatment, given later, involves substituting this polarization in the wave equation (8.65)], and this e.m. wave has the form

$$E_{2\omega}(z,t) = \tfrac{1}{2}\left\{ E(z,2\omega)\exp\left[i(2\omega t - k_{2\omega} z)\right] + \text{c.c.}\right\} \tag{8.45}$$

where

$$k_{2\omega} = \frac{2\omega}{c_{2\omega}} = \frac{2n_{2\omega}\omega}{c_0} \tag{8.46}$$

is the wavevector (magnitude) at frequency 2ω. The physical origin of SHG can thus be traced back to the fact that, as a result of the nonlinear relation (8.41), the e.m. wave at the fundamental frequency ω will beat with itself to produce a polarization at 2ω. A comparison of (8.44) with (8.45) reveals a very important condition which must be satisfied if this process is to occur efficiently, viz., that the phase velocity of the polarization wave ($v_P = 2\omega/2k_\omega$) be equal to that of the generated e.m. wave ($v_E = 2\omega/k_{2\omega}$). The condition can thus be written

$$k_{2\omega} = 2k_\omega \tag{8.47}$$

In fact, if this condition is not satisfied, the phase of the polarization wave at some point a distance l into the crystal (i.e., where the phase is $2k_\omega l$) will

†The quantity P^{NL} also contains a term at frequency $\omega = 0$ which leads to development of a dc voltage across the crystal (optical rectification).

be different from that of the generated wave (phase $k_{2\omega}l$). This increasing phase difference with distance l means that the generated wave will not grow cumulatively with distance l since it is not being driven by a polarization with the appropriate phase. Condition (8.47) is therefore referred to as the *phase-matching* condition. Note that, according to (8.43) and (8.46), equation (8.47) reduces to

$$n_{2\omega} = n_\omega \tag{8.48}$$

If the directions of E_ω and P^{NL} (and hence of $E_{2\omega}$) were indeed the same [as implied by (8.41)] it would not be possible to satisfy the condition (8.48) owing to the dispersion ($\Delta n = n_{2\omega} - n_\omega$) of the crystal. This would then set a severe limit to the crystal length l_c over which P^{NL} can give contributions which keep adding cumulatively to form the second harmonic wave. This length l_c (the coherence length) must in fact correspond to the distance over which the P wave and the $E_{2\omega}$ wave get out of phase with each other by an amount π, i.e., $k_{2\omega}l_c - 2k_\omega l_c = \pi$. From this, with the help of (8.43) and (8.46), we get

$$l_c = \frac{\lambda}{4\Delta n} \tag{8.49}$$

where $\lambda = 2\pi c_0/\omega$ is the wavelength *in vacuo* of the fundamental wave. Taking, as an example, $\lambda \simeq 1\ \mu\text{m}$ and $\Delta n = 10^{-2}$, we get $l_c = 25\ \mu\text{m}$. Note that, at this distance into the crystal, the contribution of the P wave to the $E_{2\omega}$ wave is 180° out of phase and the $E_{2\omega}$ wave thus begins to decrease rather than continuing to increase. In this case, with l_c having such a small value, only a very small fraction of the incident power can then be transformed into the second harmonic wave.

At this point it is worth pointing out another useful way of visualizing the SHG process, in terms of photons rather than fields. First we write the relation between the frequency of the fundamental (ω) and second-harmonic (ω_{SH}) wave, viz.,

$$\omega_{\text{SH}} = 2\omega \tag{8.50}$$

If we now multiply both sides of (8.47) and (8.50) by $\hbar$, we get

$$\hbar\omega_{\text{SH}} = 2\hbar\omega \tag{8.51a}$$

$$\hbar k_{2\omega} = 2\hbar k_\omega \tag{8.51b}$$

For energy to be conserved in the SHG process, we must have $dI_{2\omega}/dz = -dI_\omega/dz$, where $I_{2\omega}$ and I_ω are the wave intensities at the two frequencies. With the help of (8.51a) we get $dF_{2\omega}/dz = -2dF_\omega/dz$, where $F_{2\omega}$ and F_ω are the photon fluxes of the two waves. From this last equation we can then say that, in the SHG process, whenever two photons at frequency ω

disappear, one photon at frequency 2ω is produced. Thus the relation (8.51*a*) can be regarded as a statement of conservation of photon energy. Recalling that a photon has a momentum $\hbar k$, then equation (8.51*b*) is seen to correspond to the requirement that photon momentum also be conserved in the process.

We now reconsider the phase-matching condition (8.48) to see how it can be satisfied in a suitable, optically anisotropic crystal.[12,13] To understand this we will first need to make a small digression to explain the propagation behavior of waves in an anisotropic crystal, and also how the simple nonlinear relation (8.41) should be generalized for anisotropic media.

In an anisotropic crystal it can be shown that, for a given direction of propagation, there are two different, linearly polarized plane waves which can propagate. Corresponding to these two different polarizations there are two different refractive indices. The difference of refraction index is referred to as birefringence. This behavior is usually described in terms of the so-called index ellipsoid which, for a uniaxial crystal, is an ellipsoid of revolution around the optic axis (the z axis of Fig. 8.6). The two allowed directions of polarization and their corresponding refractive indices are found as follows: Through the center of the ellipsoid we draw a line in the direction of beam propagation (line OP of Fig. 8.6) and a plane perpendicular to this line. The intersection of this plane with the ellipsoid is an ellipse. The two axes of this ellipse are parallel to the two directions of polarization, and the length of each semiaxis is equal to the refractive index for that direction of polarization. One of these directions is necessarily perpendicular to the optic axis, and the wave having this polarization

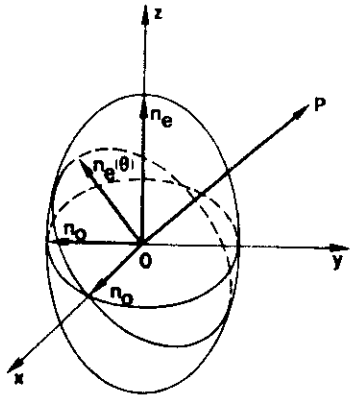

FIG. 8.6. Index ellipsoid for a positive uniaxial crystal.

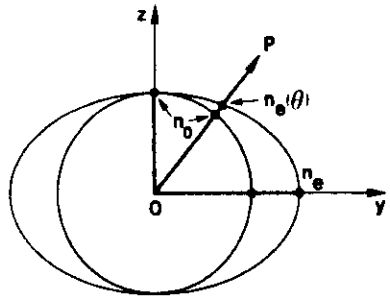

FIG. 8.7. Normal (index) surface for both the ordinary and extraordinary waves (for a positive uniaxial crystal).

direction is called the ordinary wave. Its refractive index n_0 can be seen from the figure to be independent of the direction of propagation. The wave with the other direction of polarization is called the extraordinary wave and the corresponding index $n_e(\theta)$ ranges in value from that of the ordinary wave n_0 (when OP is parallel to z) to a value n_e, called the extraordinary index (when OP is perpendicular to z). A positive uniaxial crystal corresponds to the case $n_e > n_o$, and a negative uniaxial crystal, to the case $n_e < n_0$. An equivalent way to describe wave propagation is through the so-called normal (index) surfaces for the ordinary and extraordinary waves (Fig. 8.7). In this case, for a given direction of propagation OP and for either ordinary or extraordinary waves the length of the ray OP (P being the point of interception with the surface) gives the refractive index of the wave. The normal surface for the ordinary wave is thus a sphere, while the normal surface for the extraordinary wave is an ellipsoid of revolution around the z axis. In Fig. 8.7 the intersections of these two normal surfaces with the y–z plane are indicated for the case of a positive uniaxial crystal.

After this brief discussion of wave propagation in anisotropic crystals, we now return to the problem of the induced nonlinear polarization. In general, in an anisotropic medium, the scalar relation (8.41) does not hold and a tensor relation needs to be introduced. First, we write the electric field $\mathbf{E}^{\omega}(r,t)$ of the e.m. wave at frequency ω and at a given point $\mathbf{r}$ and the nonlinear polarization vector at frequency 2ω, $\mathbf{P}_{\mathrm{NL}}^{2\omega}(r,t)$, in the form

$$\mathbf{E}^{\omega}(\mathbf{r},t) = \tfrac{1}{2}\left[\mathbf{E}^{\omega}(\mathbf{r},\omega)\exp(i\omega t) + \text{c.c.}\right] \tag{8.52a}$$

$$\mathbf{P}_{\mathrm{NL}}^{2\omega}(\mathbf{r},t) = \tfrac{1}{2}\left[\mathbf{P}^{2\omega}(\mathbf{r},2\omega)\exp(2i\omega t) + \text{c.c.}\right] \tag{8.52b}$$

A tensor relation can then be established between $\mathbf{P}^{2\omega}(\mathbf{r},2\omega)$ and $\mathbf{E}^{\omega}(\mathbf{r},\omega)$. The second harmonic polarization component along, say, the i direction of

the crystal can be written as

$$P_i^{2\omega} = \sum_{j,k=1,2,3} \varepsilon_0 d_{ijk}^{2\omega} E_j^{\omega} E_k^{\omega} \tag{8.53}$$

Note that (8.53) is often written in condensed notation as

$$P_i^{2\omega} = \sum_{1}^{6} {}_m \varepsilon_0 d_{im}^{2\omega} (EE)_m \tag{8.54}$$

where m runs from 1 to 6. The abbreviated field notation is that $(EE)_1 \equiv E_1^2 \equiv E_x^2$, $(EE)_2 \equiv E_2^2 \equiv E_y^2$, $(EE)_3 \equiv E_3^2 \equiv E_z^2$, $(EE)_4 \equiv 2E_2E_3 \equiv 2E_yE_z$, $(EE)_5 \equiv 2E_1E_3 \equiv 2E_xE_z$, and $(EE)_6 \equiv 2E_1E_2 \equiv 2E_xE_y$, where both the 1, 2, 3 and the x, y, z notation for axes have been indicated. Note that, expressed in matrix form, d_{im} is a 3×6 matrix which operates on the column vector $(EE)_m$. Depending on the crystal symmetry, some of the values of the d_{im} matrix may be equal and some may be zero. For the $\bar{4}2m$ point group symmetry, which includes the important nonlinear crystals of the KDP type and the chalcopyrite semiconductors, only d_{14}, d_{25}, and d_{36} are nonzero and these three d coefficients are themselves equal. Thus only one coefficient, for example, d_{36}, needs to be specified, and we can write

$$P_x = 2\varepsilon_0 d_{36} E_y E_z \tag{8.55a}$$

$$P_y = 2\varepsilon_0 d_{36} E_z E_x \tag{8.55b}$$

$$P_z = 2\varepsilon_0 d_{36} E_x E_y \tag{8.55c}$$

where the z axis is again taken along the optic axis of the uniaxial crystal. The nonlinear optical coefficients, the symmetry class, and the transparency range of some selected nonlinear materials are indicated in Table 8.1.

Following this digression on the properties of anisotropic media, we can now go on to show how phase matching can be achieved for the particular case of a crystal of $\bar{4}2m$ point group symmetry. From (8.55) we note that, if $E_z = 0$, only P_z will be nonvanishing and will thus tend to generate a second-harmonic wave with a nonzero z component. We recall (see Fig. 8.6) that a wave with $E_z = 0$ is an ordinary wave while a wave with $E_z \neq 0$ is an extraordinary wave. Thus an ordinary wave at the fundamental frequency ω tends, in this case, to generate an extraordinary wave at 2ω. To satisfy the phase-matching condition one can then propagate the fundamental wave at an angle θ_m to the optic axis, in such a way that

$$n_e(2\omega, \theta_m) = n_0(\omega) \tag{8.56}$$

This can be better understood with the help of Fig. 8.8 which shows the intercepts of the normal surfaces $n_o(\omega)$ and $n_e(2\omega, \theta)$ with the plane containing the z axis and the propagation direction. Note that, due to dispersion

TABLE 8.1. Nonlinear Optical Coefficients for Selected Materials

Material	Symbol	Formula	Nonlinear d coefficient (relative to KDP)	Symmetry class	Transparence range (μm)
Potassium dihydrogen phosphate	KDP	KH_2PO_4	$d_{36} = d_{14} = 1$	$\bar{4}2m$	0.22–1.1
Potassium dideuterium phosphate	KD*P	KD_2PO_4	$d_{36} = d_{14} = 1.06$	$\bar{4}2m$	0.22–1.1
Ammonium dihydrogen phosphate	ADP	$NH_4H_2PO_4$	$d_{36} = d_{14} = 1.2$	$\bar{4}2m$	0.2–1.1
Cesium dihydrogen arsenate	CDA	CsH_2AsO_4	$d_{36} = d_{14} = 0.92$	$\bar{4}2m$	0.26–1.6
Lithium iodate	—	$LiIO_3$	$d_{31} = d_{32} = d_{24} = d_{15} = 14$	6	0.31–5.5
Cadmium germanium arsenide	—	$CdGeAs_3$	$d_{36} = d_{14} = 472$	$\bar{4}2m$	2–20
Lithium niobate		$LiNbO_3$	$d_{31} = 10.6$ $d_{22} = 5.1$	$3m$	0.35–4.5
Proustite		Ag_3AsS_3	$d_{31} = 30$ $d_{22} = 50$	$3m$	0.6–13

(normal dispersion), we have $n_o(\omega) < n_o(2\omega) = n_e(2\omega, 0)$. Thus the ordinary circle (for frequency ω) intersects the extraordinary ellipse (for frequency 2ω) at some angle θ_m.† For light propagating at this angle θ_m to the optic axis (i.e., for all ray directions lying in a cone around the z axis, with cone angle θ_m), equation (8.56) is satisfied and hence the phase-matching condition is satisfied. Note, however, that if $\theta \neq 90°$, the phenomenon of double refraction will occur, i.e., the direction of the energy flow for the extraordinary (SH) beam will be at an angle slightly different from θ_m. Thus the fundamental and SH beams will travel in slightly different directions (although satisfying the phase-matching condition). For a fundamental beam of finite transverse dimensions this will put an upper limit on the interaction length in the crystal. This limitation can be overcome if it is

†It should be noted that for this intersection to occur at all it is necessary for $n_e(2\omega, 90°)$ to be less than $n_o(\omega)$, otherwise the ellipse for $n_e(2\omega)$ (see Fig. 8.8) will lie wholly outside the circle for $n_o(\omega)$. Thus $n_e(2\omega, 90°) = n_e(2\omega) < n_o(\omega) < n_o(2\omega)$ which shows that crystal birefringence $n_o(2\omega) - n_e(2\omega)$ must be larger than crystal dispersion $n_o(2\omega) - n_o(\omega)$.

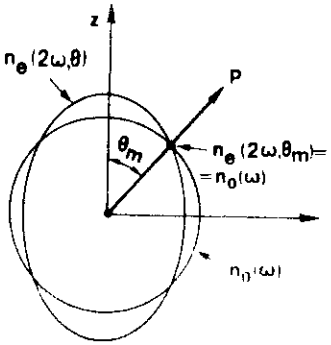

FIG. 8.8. Phase-matching angle θ_m for type I second-harmonic generation in a negative uniaxial crystal.

possible to operate with $\theta_m = 90°$, i.e., $n_e(2\omega, 90°) = n_o(\omega)$. This kind of phase matching is called 90° phase matching and in some cases can be achieved by changing the crystal temperature, since n_o and n_e in general undergo different changes with the temperature. To summarize the above discussion, we can say that phase matching can be achieved in a (sufficiently birefringent) negative uniaxial crystal when an ordinary ray at ω [E_x beam of (8.55*c*)] combines with an ordinary ray at ω [E_y beam of (8.55*c*)] to give an extraordinary ray at 2ω, or, in symbols, $o_\omega + o_\omega \rightarrow e_{2\omega}$. This is called type I second-harmonic generation. In a negative uniaxial crystal another scheme for phase-matched SHG, called type II, is also possible. In this case an ordinary wave at ω can combine with an extraordinary wave at ω to give an extraordinary wave at 2ω, or, in symbols, $o_\omega + e_\omega \rightarrow e_{2\omega}$.†

Second-harmonic generation is currently used to provide coherent sources at new wavelengths. The nonlinear crystal may be placed either outside or inside the cavity of the laser producing the fundamental beam. In the latter case one takes advantage of the greater e.m. field strength inside the resonator to increase the conversion efficiency. Very high conversion efficiencies (approaching 100%) have been obtained with both arrangements. Among the most frequent applications of SHG are frequency doubling the output of a Nd:YAG laser (thus producing a green beam, $\lambda = 532$ nm, from an infrared one, $\lambda = 1.06$ μm) and generation of tunable UV radiation (down to $\lambda = 210$ nm) by frequency doubling a tunable dye laser. In both of these cases either cw or pulsed laser sources are used.

†More generally, interactions in which the polarizations of the two fundamental waves are the same are termed type I (e.g., also $e_\omega + e_\omega \rightarrow o_{2\omega}$), and interactions in which the polarization of the fundamental waves are orthogonal are termed type II.

The nonlinear crystals most commonly used for SHG belong to the $\bar{4}2m$ point group symmetry, in particular the materials KDP, KD*P, and CDA. For intracavity SHG, Lithium Iodate ($LiIO_3$) is also often used. Efficient frequency conversion of infrared radiation from CO_2 or CO lasers in chalcopyrite semiconductors (e.g., $CdGeAs_2$) is another interesting example.

8.4.1.2 Parametric Oscillation

We now go on to discuss the process of parametric oscillation. We begin by noticing that the previous ideas introduced in the context of SHG can be readily extended to the case of two incoming waves at frequencies ω_1 and ω_2 combining to give a wave at frequency $\omega_3 = \omega_1 + \omega_2$ (sum-frequency generation). Harmonic generation can in fact be thought of as a limiting case of sum-frequency generation with $\omega_1 = \omega_2 = \omega$ and $\omega_3 = 2\omega$. The physical picture is again very similar to the SHG case: By virtue of the nonlinear relation (8.41) between P^{NL} and the total field E [$E = E_{\omega_1}(z,t) + E_{\omega_2}(z,t)$], the wave at ω_1 will beat with that at ω_2 to give a polarization component at $\omega_3 = \omega_1 + \omega_2$. This will then radiate an e.m. wave at ω_3. Thus for sum-frequency generation we can write

$$\hbar\omega_1 + \hbar\omega_2 = \hbar\omega_3 \tag{8.57a}$$

which, according to a description in terms of photons rather than fields, implies that one photon at ω_1 and one photon at ω_2 disappear while a photon at ω_3 is created. We therefore expect the photon momentum to be also conserved in the process, i.e.,

$$\hbar\mathbf{k}_1 + \hbar\mathbf{k}_2 = \hbar\mathbf{k}_3 \tag{8.57b}$$

where the relationship is put in its general form, with the k denoted by vectors. Equation (8.57*b*), which expresses the phase-matching condition for sum-frequency generation, can be seen to be a straightforward generalization of that for SHG [compare with (8.51*b*)].

Optical parametric generation is in fact just the reverse of sum-frequency generation. Here a wave at frequency ω_3 (the pump frequency) generates two waves (called the idler and signal waves) at frequencies ω_1 and ω_2, in such a way that the total photon energy and momentum is conserved, i.e.,

$$\hbar\omega_3 = \hbar\omega_1 + \hbar\omega_2 \tag{8.58a}$$

$$\hbar\mathbf{k}_3 = \hbar\mathbf{k}_1 + \hbar\mathbf{k}_2 \tag{8.58b}$$

The physical process occurring in this case can be visualized in the

following way. Imagine first that a strong wave at ω_3 and a weak wave at ω_1 are both present in the nonlinear crystal. As a result of the nonlinear relation (8.41), the wave at ω_3 will beat with the wave at ω_1 to give a polarization component at $\omega_3 - \omega_1 = \omega_2$. If the phase-matching condition (8.58*b*) is satisfied, a wave at ω_2 will thus build up as it travels through the crystal. Then the total E field will in fact be the sum of three fields $[E = E_{\omega_1}(z,t) + E_{\omega_2}(z,t) + E_{\omega_3}(z,t)]$ and the wave at ω_2 will in turn beat with the wave at ω_3 to give a polarization component at $\omega_3 - \omega_2 = \omega_1$. This polarization will cause the ω_1 wave to grow also. Thus power will be transferred from the beam at ω_3 to those at ω_1 and ω_2, and the weak wave at ω_1 which was assumed to be initially present will be amplified. From this picture we see a fundamental difference between parametric generation and SHG. In the latter case only a strong beam at the fundamental frequency is needed for the SHG process to occur. In the former case, however, a weak beam at ω_1 is also needed and the system behaves like an amplifier at frequency ω_1 (and ω_2). In practice, however, the weak beam need not be supplied by an external source (such as another laser) since it is generated internally to the crystal as a form of noise (so-called parametric noise). One can then generate coherent beams from this noise in a way analogous to that used in a laser oscillator. Thus, the nonlinear crystal, which is pumped by an appropriately focused pump beam, is placed in an optical resonator (Fig. 8.9). The two mirrors (1 and 2) of this parametric oscillator have high reflectivity (e.g., $R_1 = 1$ and $R_2 \simeq 1$) either at ω_1 only (singly resonant oscillator, SRO) or at both ω_1 and ω_2 (doubly resonant oscillator, DRO). The mirrors are ideally transparent to the pump beam. Oscillation will start when the gain arising from the parametric effect just exceeds the losses of the optical resonator. Some threshold power of the input pump beam is therefore required before oscillation will begin. When this threshold is reached, oscillation occurs at both ω_1 and ω_2, and the particular pair of values of ω_1 and ω_2 is determined by the two equations (8.58). For instance, with type I phase matching involving an extraordinary wave at ω_3 and

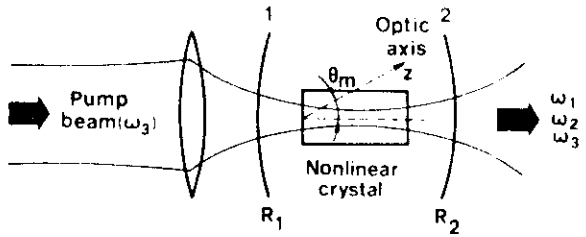

FIG. 8.9. Schematic diagram of an optical parametric oscillator.

ordinary waves at ω_1 and ω_2 (i.e., $e_{\omega_3} \rightarrow o_{\omega_1} + o_{\omega_2}$) in (8.58*b*) would give

$$\omega_3 n_e(\omega_3, \theta) = \omega_1 n_o(\omega_1) + \omega_2 n_o(\omega_2) \tag{8.59}$$

For a given θ, i.e., for a given inclination of the nonlinear crystal with respect to the cavity axis, (8.59) provides a relation between ω_1 and ω_2 which, together with the relation (8.58*a*), determines the values of both ω_1 and ω_2. Phase-matching schemes of both type I and type II (e.g., $e_{\omega_3} \rightarrow o_{\omega_1} + e_{\omega_2}$ for a negative uniaxial crystal) are possible and tuning can be achieved by either changing the crystal inclination (angle tuning) or its temperature (temperature tuning). As a final comment, we note that, if the gain from the parametric effect is large enough, one can dispense with the mirrors altogether, and an intense emission at ω_1 and ω_2 grows from parametric noise in a single pass through the crystal. This behavior is superficially rather similar to the phenomena of superfluorescence and amplified spontaneous emission discussed in Section 2.3.4 and is sometimes (rather inappropriately) called superfluorescent parametric emission.

Singly resonant and doubly resonant optical parametric oscillators have both been used. Doubly resonant parametric oscillation has been achieved with both cw and pulsed pump lasers. For cw excitation, threshold powers as low as a few milliwatts have been demonstrated. However, the doubly resonant character of the resonator causes the output to be somewhat unstable both in amplitude and frequency. Singly resonant parametric oscillation has only been achieved using pulsed pump lasers since the threshold pump power for the singly resonant case is much higher (as much as about two orders of magnitude) than that of the doubly resonant case. However, singly resonant oscillators produce a much more stable output and impose less stringent demands on the mirror coating design. For these reasons the singly resonant configuration is the one most frequently used. Optical parametric oscillators producing coherent radiation from the visible to the near infrared (0.5–3.5 μm) are now well developed, with the most successful device based on a lithium niobate ($LiNbO_3$) crystal pumped by a Nd:YAG laser. They face competition, however, from color-center lasers, which operate in a similar range in the infrared. Optical parametric oscillators can also generate coherent radiation at longer infrared wavelengths (to $\sim$14 μm) using crystals such as proustite (Ag_3AsS_3) and cadmium selenide (CdSe).† The efficiency of an OPO can also be very high (approaching the theoretical 100% photon efficiency).

†Materials such as the chalcopyrite semiconductors have shown much promise, but unfortunately suffer from high loss and hence have not been operated as parametric oscillators. Nevertheless, these materials and many others have been widely used for difference frequency generation, i.e., where two beams, ω_3 and ω_1, are used to generate radiation at their difference frequency $\omega_2 = \omega_3 - \omega_1$.

8.4.2 Analytical Treatment

To arrive at an analytical description of both SHG and parametric processes, we need to see how the nonlinear polarization [e.g., (8.41)] which acts as the source term to drive the generated waves is introduced into the wave equation. The fields within the material obey Maxwell's equations:

$$\nabla \times \mathbf{E} = -\frac{\partial \mathbf{B}}{\partial t} \tag{8.60a}$$

$$\nabla \times \mathbf{H} = \mathbf{J} + \frac{\partial \mathbf{D}}{\partial t} \tag{8.60b}$$

$$\nabla \cdot \mathbf{D} = \rho \tag{8.60c}$$

$$\nabla \cdot \mathbf{B} = 0 \tag{8.60d}$$

where ρ is the free-charge density. For the media of interest here we can assume the magnetization $\mathbf{M}$ to be zero; thus

$$\mathbf{B} = \mu_0 \mathbf{H} + \mu_0 \mathbf{M} = \mu_0 \mathbf{H} \tag{8.61}$$

Losses within the material (e.g., scattering losses) can be simulated by the introduction of a fictitious conductivity σ_s such that

$$\mathbf{J} = \sigma_s \mathbf{E} \tag{8.62}$$

Finally we can write

$$\mathbf{D} = \epsilon_0 \mathbf{E} + \mathbf{P}^{\mathrm{L}} + \mathbf{P}^{\mathrm{NL}} = \epsilon \mathbf{E} + \mathbf{P}^{\mathrm{NL}} \tag{8.63}$$

where $\mathbf{P}^{\mathrm{L}}$ is the linear polarization of the medium and is taken account of, in the usual way, by introducing the dielectric constant ϵ. As we shall now see, when $\mathbf{D}$ given by (8.63) is substituted in Maxwell's equations, the nonlinear polarization term $\mathbf{P}^{\mathrm{NL}}$ is introduced into the wave equation. Applying the $\nabla \times$ operator to both sides of (8.60*a*) [interchanging the order of $\nabla \times$ and $\partial/\partial t$ operators on the right-hand side of (8.60*a*)] and making use of (8.61), (8.60*b*), (8.62), and (8.63), we first obtain

$$\nabla \times \nabla \times \mathbf{E} = -\mu_0 \left(\sigma_s \frac{\partial \mathbf{E}}{\partial t} + \epsilon \frac{\partial^2 \mathbf{E}}{\partial t^2} + \frac{\partial^2 \mathbf{P}^{\mathrm{NL}}}{\partial t^2} \right) \tag{8.64}$$

Using the identity $\nabla \times \nabla \times \mathbf{E} = (\nabla \cdot \mathbf{E}) - \nabla^2 \mathbf{E}$ and making the assumption that $\nabla \cdot \mathbf{E} \simeq 0$, we find from (8.64) that

$$\nabla^2 \mathbf{E} - \frac{\sigma_s}{\epsilon c^2} \frac{\partial \mathbf{E}}{\partial t} - \frac{1}{c^2} \frac{\partial^2 \mathbf{E}}{\partial t^2} = \frac{1}{\epsilon c^2} \frac{\partial^2 \mathbf{P}^{\mathrm{NL}}}{\partial t^2} \tag{8.65}$$

where $c = (\epsilon \mu_0)^{-1/2}$ is the phase velocity in the material. Equation (8.65) is the wave equation with the nonlinear polarization term included. Note that the linear part of the medium polarization has been transferred to the left-hand side of (8.65) and is contained in the dielectric constant ϵ. The

nonlinear part $\mathbf{P}^{\mathrm{NL}}$ has been kept on the right-hand side, and it will be shown to act as a source term for the waves being generated at new frequencies as well as a loss term for the incoming wave. Confining ourselves to the simple scalar case of plane waves propagating along the z direction, we see that (8.65) reduces to

$$\frac{\partial^2 E}{\partial z^2} - \frac{\sigma_s}{\epsilon c^2} \frac{\partial E}{\partial t} - \frac{1}{c^2} \frac{\partial^2 E}{\partial t^2} = \frac{1}{\epsilon c^2} \frac{\partial^2 \mathbf{P}^{\mathrm{NL}}}{\partial t^2} \tag{8.65a}$$

The field amplitude at frequency ω_j will be written as

$$E^{\omega_j}(z,t) = \tfrac{1}{2}\{E_j(z) \exp[i(\omega_j t - k_j z)] + \text{c.c.}\} \tag{8.66a}$$

where E_j is taken to be complex in general. Likewise, the amplitude of the nonlinear polarization at frequency ω_j will be written as

$$\mathbf{P}^{\mathrm{NL}}_{\omega_j} = \tfrac{1}{2}\{\mathbf{P}^{\mathrm{NL}}_j(z) \exp[i(\omega_j t - k_j z)] + \text{c.c.}\} \tag{8.66b}$$

Since (8.65*a*) must hold separately for each frequency corresponding to waves which are present in the crystal, equations (8.66*a*) and (8.66*b*) can be substituted into the left- and right-hand sides of (8.65*a*) respectively. Within the slowly varying amplitude approximation, we can neglect the second derivative of $E_j(z)$ (i.e., assume that $d^2E_j/dz^2 \ll k_j dE_j/dz$), and (8.65*a*) then yields

$$2\frac{dE_j}{dz} + \frac{\sigma_j}{n_j \epsilon_0 c_0} E_j = -i\left(\frac{\omega_j}{n_j \epsilon_0 c_0}\right) \mathbf{P}^{\mathrm{NL}}_j \tag{8.67}$$

where the relations $k_j = n_j \omega_j / c_0$ and $\epsilon_j = n_j^2 \epsilon_0$ have been used (c_0 is the light velocity *in vacuo* and n_j is the refractive index at ω_j).

Equation (8.67) is the basic equation that will be used in the next sections. Note that it has been obtained subject to the assumption of a scalar relation between $\mathbf{P}^{\mathrm{NL}}$ and $\mathbf{E}$ [see (8.41)]. This assumption is not correct, and actually a tensor relation should be used [see (8.54)]. However, it can be shown that one can still use this scalar equation provided that E_j now refers to the field component along an appropriate axis and an effective coefficient, d_{eff}, is substituted for d in (8.41). In general, d_{eff} is a combination of one or several of the d_{im} coefficients appearing in (8.54) and of the angles θ and ϕ which define the direction of wave propagation in the crystal[14] (θ is the angle to the z axis and ϕ is the angle that the projection of the propagation vector in the x–y plane makes with the x axis of the crystal). For example, for a crystal of $\bar{4}2m$ point group symmetry and for type I phase matching, one obtains $d_{\mathrm{eff}} = d_{36} \sin 2\phi \sin\theta$. As a short-hand notation, however, we will still retain the symbol d in (8.41) while bearing in mind that it means the effective value of the d coefficient, d_{eff}.

8.4.2.1 *Parametric Oscillation*

We now consider three waves at frequencies ω_1, ω_2, and ω_3 [where $\omega_3 = \omega_1 + \omega_2$] interacting in the crystal. We thus write the total field $E(z,t)$ as

$$E(z,t) = E^{\omega_1}(z,t) + E^{\omega_2}(z,t) + E^{\omega_3}(z,t) \tag{8.68}$$

where each of the fields can be written in the form of (8.66*a*). Upon substituting (8.68) into (8.41) and using (8.66*a*) we obtain an expression for the components $P_j^{\mathrm{NL}}(z)$ [as defined by (8.66*b*)] of the nonlinear polarization at the various frequencies ω_j. After some lengthy but straightforward algebra we find that, for instance, the component P_1^{NL} at frequency ω_1 is given by

$$P_1^{\mathrm{NL}} = 2\varepsilon_0 d E_3(z) E_2^*(z) \exp\left[i(k_1 + k_2 - k_3)z\right] \tag{8.69}$$

The components of P^{NL} at ω_2 and ω_3 are obtained in a similar way. The field equations for each of the three frequencies are then obtained by substituting the appropriate P^{NL} into (8.67). We thus arrive at the following three equations:

$$\frac{dE_1}{dz} = -\left(\frac{\sigma_1}{2n_1\varepsilon_0 c_0}\right)E_1 - i\left(\frac{\omega_1}{n_1 c_0}\right) d E_3 E_2^* \exp\left[-i(k_3 - k_2 - k_1)z\right] \tag{8.70a}$$

$$\frac{dE_2}{dz} = -\left(\frac{\sigma_2}{2n_2\varepsilon_0 c_0}\right)E_2 - i\left(\frac{\omega_2}{n_2 c_0}\right) d E_3 E_1^* \exp\left[-i(k_3 - k_1 - k_2)z\right] \tag{8.70b}$$

$$\frac{dE_3}{dz} = -\left(\frac{\sigma_3}{2n_3\varepsilon_0 c_0}\right)E_3 - i\left(\frac{\omega_3}{n_3 c_0}\right) d E_1 E_2 \exp\left[-i(k_1 + k_2 - k_3)z\right] \tag{8.70c}$$

These are the basic equations describing the nonlinear parametric interaction. We note that they are coupled to each other via the nonlinear coefficient d.

It is convenient at this point to define new field variables A_j as

$$A_j = (n_j/\omega_j)^{1/2} E_j \tag{8.71}$$

Since the intensity of the wave is $I_j = n_j\varepsilon_0 c_0 |E_j|^2/2$, the corresponding photon flux F_j is $F_j = I_j/\hbar\omega_j = (\varepsilon_0 c_0/2\hbar)|A_j|^2$. Thus $|A_j|^2$ is proportional to the photon flux at ω_j with the proportionality constant being independent of n_j and ω_j. When re-expressed in terms of these new field variables, equations (8.70) transform to

$$\frac{dA_1}{dz} = -\frac{\alpha_1 A_1}{2} - i\lambda A_3 A_2^* \exp\left[-i(\Delta k z)\right] \tag{8.72a}$$

$$\frac{dA_2}{dz} = -\frac{\alpha_2 A_2}{2} - i\lambda A_3 A_1^* \exp\left[-i(\Delta k z)\right] \tag{8.72b}$$

$$\frac{dA_3}{dz} = -\frac{\alpha_3 A_3}{2} - i\lambda A_1 A_2 \exp\left[i(\Delta k z)\right] \tag{8.72c}$$

where we have put $\alpha_j = \sigma_j/n_j\varepsilon_0 c_0$, $\Delta k = k_3 - k_2 - k_1$, and

$$\lambda = \frac{d}{c_0}\left[\frac{\omega_1\omega_2\omega_3}{n_1 n_2 n_3}\right]^{1/2} \tag{8.73}$$

The advantage of using A_j instead of E_j is now apparent since, unlike (8.70), relations (8.72) now involve a single coupling parameter λ.

Neglecting the losses (i.e., putting $\alpha_j = 0$), multiplying both sides of (8.72*a*) by A_1^* and both sides of (8.72*b*) by A_2^*, and comparing the resulting expressions, we arrive at the following relation: $d|A_1|^2/dz = d|A_2|^2/dz$. Similarly from (8.72*b*) and (8.72*c*) we get $d|A_2|^2/dz = -d|A_3|^2/dz$. We can therefore write

$$\frac{d|A_1|^2}{dz} = \frac{d|A_2|^2}{dz} = -\frac{d|A_3|^2}{dz} \tag{8.74}$$

which are known as the Manley–Rowe relations. Since $|A_j|^2$ is proportional to the corresponding photon flux, (8.74) implies that whenever a photon at ω_3 is destroyed, a photon at ω_1 and a photon at ω_2 are created. This is consistent with the photon model for the parametric process, as discussed in Section 8.4.1.2. Note that (8.74) means, for instance, that $(dP_1/dz) = -(\omega_1/\omega_3)(dP_3/dz)$, where P_1 and P_3 are the powers of the two waves. Thus only the fraction (ω_1/ω_3) of the power at frequency ω_3 can be converted into that at frequency ω_1.

Strictly speaking, equations (8.72) apply to a traveling wave situation in which an arbitrarily long crystal is being traversed by the three waves at ω_1, ω_2, ω_3. We now want to see how these equations might be applied to the case of an optical parametric oscillator as in Fig. 8.9. Here we will first consider the DRO scheme. The waves at ω_1 and ω_2 will therefore travel back and forth within the cavity, and the parametric process will only occur when their propagation direction is the same as that of the pump wave (since it is only under these circumstances that phase matching can be satisfied). If we unfold the optical path, it will look like that of Fig. 8.10a, and it can be seen that loss occurs on every pass while parametric gain

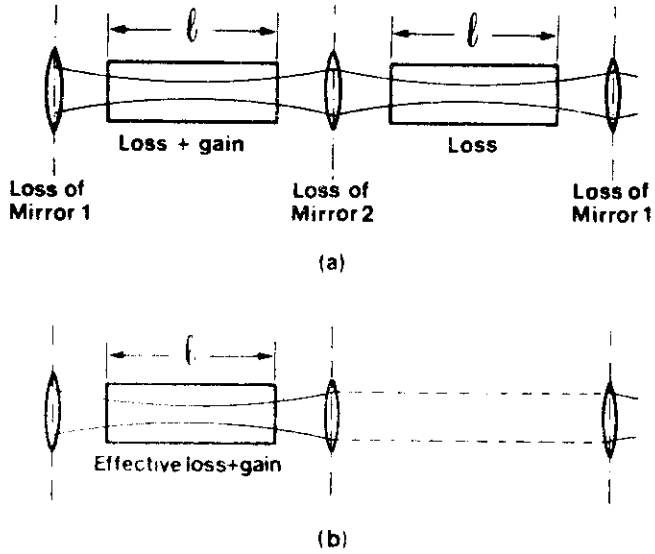

FIG. 8.10. (a) Unfolded path of an optical parametric oscillator; (b) Reduction to a single-pass scheme with mirror losses incorporated into the distributed losses of the crystal.

occurs only once in every two passes. This situation can be reduced to that of Fig. 8.10b if we choose an appropriate definition of the effective loss coefficient α_j ($j = 1, 2$). The loss due to a crystal of length l in Fig. 8.10b must in fact equal the losses incurred in a double pass in Fig. 8.10a. The latter losses must account for the actual losses in the crystal, as well as the mirror and diffraction losses. Thus the coefficients α_1 and α_2 in (8.72) must be appropriately defined so as to incorporate these various losses. From (8.72), neglecting the parametric interaction [i.e., setting $\lambda = 0$], we see that after traversing the length l of the crystal, the power at ω_j ($j = 1, 2$) is reduced to a fraction $\exp(-\alpha_j l)$ of its power at the entrance face of the crystal. This reduction must account for the round-trip cavity losses, which requires that

$$\exp(-\alpha_j l) = R_{1j} R_{2j} (1 - T)^2 \tag{8.74a}$$

where R_{1j} and R_{2j} are the two mirror reflectivities and T is the crystal loss (plus diffraction loss) per pass at ω_j. If we now define [compare with (5.4)] $\gamma_{1j} = -\ln R_{1j}$, $\gamma_{2j} = -\ln R_{2j}$, $\gamma_j' = -\ln(1 - T)$, and $\gamma_j = [(\gamma_{1j} + \gamma_{2j})/2] + \gamma_j'$, we can rewrite (8.74$a$) as

$$\alpha_j l = 2\gamma_j \tag{8.75}$$

where γ_j is the overall cavity loss per pass. Note that this amounts to simulating the mirror losses by losses distributed through the crystal and then including them in the effective crystal absorption coefficient α_j ($j = 1$, 2). The loss α_3, on the other hand, only involves crystal losses and can in general be neglected. Thus at this point we can say that, for a DRO, equations (8.72) will still apply provided that α_1 and α_2 are given by (8.75). To obtain the threshold condition of a DRO, equations (8.72) can be further simplified if we neglect depletion of the pump wave by the parametric process. This assumption together with the assumption $\alpha_3 = 0$ means that we can take $A_3(z) \simeq A_3(0)$, where $A_3(0)$, the field amplitude of the incoming pump wave, is taken to be real. With the further assumption of $\Delta k = 0$ (perfect phase matching), (8.72) is considerably simplified and becomes

$$\frac{dA_1}{dz} = -\frac{\alpha_1 A_1}{2} - i\frac{g}{2} A_2^* \tag{8.76a}$$

$$\frac{dA_2}{dz} = -\frac{\alpha_2 A_2}{2} - i\frac{g}{2} A_1^* \tag{8.76b}$$

where

$$g = 2\lambda A_3(0) = 2d\frac{E_3(0)}{c_0}\left(\frac{\omega_1\omega_2}{n_1 n_2}\right)^{1/2} \tag{8.77}$$

The threshold condition for a DRO is then readily obtained from (8.76) by putting $dA_1/dz = dA_2/dz = 0$. This leads to

$$\alpha_1 A_1 + igA_2^* = 0 \tag{8.78a}$$

$$igA_1 - \alpha_2 A_2^* = 0 \tag{8.78b}$$

where the complex conjugate of (8.76b) has been taken. The solution of this homogeneous system of equations will yield nonzero values for A_1 and A_2 only if

$$g^2 = \alpha_1\alpha_2 = 4\frac{\gamma_1\gamma_2}{l^2} \tag{8.79}$$

where (8.75) has been used. According to (8.77), g^2 is proportional to $E_3^2(0)$, i.e., to the intensity of the pump wave. Thus condition (8.79) means that a certain threshold intensity of the pump wave is needed in order for parametric oscillation to start. This intensity is proportional to the product of the single-pass (power) losses, γ_1 and γ_2, of the two waves at ω_1 and ω_2, and inversely proportional to d^2 and l^2.

The SRO case is somewhat more involved. If the laser cavity is resonant only at ω_1, then α_1 can again be written as in (8.75). Since the

wave at ω_2 is no longer reflected back through the crystal, α_2 will involve only the crystal losses and it can therefore be neglected. Again, neglecting depletion of the pump wave and assuming perfect phase matching, (8.76) will still be applicable provided we now set $\alpha_2 = 0$. For small parametric conversion we can put $A_1^*(z) \simeq A_1^*(0)$ on the right-hand side of (8.76*b*). We thus get

$$A_2(z) = -igA_1^*(0)z/2 \tag{8.80}$$

where the condition $A_2(0) = 0$ has been assumed (i.e., no field at ω_2 is fed back into the crystal by the resonator). If we substitute (8.80) in (8.76*a*) and put $A_1(z) \simeq A_1(0)$ in the right side of (8.76*a*), we get

$$\frac{dA_1}{dz} = \left[-\frac{\alpha_1}{2} + \frac{g^2 z}{4} \right] A_1(0) \tag{8.81}$$

Integration of (8.81) gives

$$A_1(l) = A_1(0)\left[1 - \frac{\alpha_1 l}{2} + \frac{g^2 l^2}{8} \right] \tag{8.82}$$

for the field at ω_1 after traversing the length l of the crystal. The threshold condition is reached when $A_1(l) = A_1(0)$, i.e., when

$$g^2 = \frac{4\alpha_1}{l} = \frac{8\gamma_1}{l^2} \tag{8.83}$$

Since g^2 is proportional to the intensity I of the pump wave, a comparison of (8.83) with (8.79) gives the ratio of threshold pump intensities as

$$\frac{I_{\text{SRO}}}{I_{\text{DRO}}} = \frac{2}{\gamma_2} \tag{8.84}$$

If, for example, we take a loss per pass of $\gamma_2 = 2\%$, we find from (8.84) that the threshold power for SRO is 100 times larger than that for DRO.

8.4.2.2 *Second-Harmonic Generation*

In the case of SHG we take

$$E(z,t) = \tfrac{1}{2}\{ E_\omega \exp[i(\omega t - k_\omega z)] + E_{2\omega} \exp[i(2\omega t - k_{2\omega} z)] + \text{c.c.} \} \tag{8.85}$$

$$P^{\text{NL}}(z,t) = \tfrac{1}{2}\{ P_\omega^{\text{NL}} \exp[i(\omega t - k_\omega z)] + P_{2\omega}^{\text{NL}} \exp[i(2\omega t - k_{2\omega} z)] + \text{c.c.} \} \tag{8.86}$$

Substituting (8.85) and (8.86) into (8.41) gives

$$P_{2\omega}^{\text{NL}} = \varepsilon_0 d E_\omega^2 \exp[-i(2k_\omega - k_{2\omega})z] \tag{8.87a}$$

$$P_\omega^{\text{NL}} = 2\varepsilon_0 d E_{2\omega} E_\omega^* \exp[-i(k_{2\omega} - 2k_\omega)z] \tag{8.87b}$$

Then, substituting (8.87) into (8.67) and neglecting crystal loses (i.e., putting $\sigma_j = 0$), we get

$$\frac{dE_{2\omega}}{dz} = -i\frac{\omega}{n_{2\omega}c_0} d E_\omega^2 \exp(i\Delta k z) \tag{8.88a}$$

$$\frac{dE_\omega}{dz} = -i\frac{\omega}{n_\omega c_0} d E_{2\omega} E_\omega^* \exp(-i\Delta k z) \tag{8.88b}$$

where $\Delta k = k_{2\omega} - 2k_\omega$. These are the basic equations describing SHG. To solve them, it is first convenient to define new field variables E'_ω and $E'_{2\omega}$ such that

$$E'_\omega = (n_\omega)^{1/2} E_\omega \tag{8.89a}$$

$$E'_{2\omega} = (n_{2\omega})^{1/2} E_{2\omega} \tag{8.89b}$$

Since the intensity I_ω of the wave at ω is proportional to $n_\omega |E_\omega|^2$, the quantity $|E'_\omega|^2$ is also proportional to I_ω but with the proportionality constant independent of refractive index. Substituting (8.89) into (8.88) gives

$$\frac{dE'_{2\omega}}{dz} = -\frac{i}{l_{\text{SH}}} \frac{E_\omega'^2}{E'_\omega(0)} \exp[i(\Delta k z)] \tag{8.90a}$$

$$\frac{dE'_\omega}{dz} = -\frac{i}{l_{\text{SH}}} \frac{E'_{2\omega} E_\omega'^*}{E'_\omega(0)} \exp[-i(\Delta k z)] \tag{8.90b}$$

where $E'_\omega(0)$ is the value of E'_ω at $z = 0$ and l_{SH} is a characteristic length for the second-harmonic interaction, given by

$$l_{\text{SH}} = \frac{\lambda_0 (n_\omega n_{2\omega})^{1/2}}{2\pi d E_\omega(0)} \tag{8.91}$$

where λ_0 is the wavelength and $E_\omega(0)$ the incident field amplitude of the fundamental wave at frequency ω. Note again that the advantage of using the new field variables E'_ω and $E'_{2\omega}$ is apparent from equations (8.90) since they involve a single coupling parameter l_{SH}. Note also that $E_\omega(0)$ and hence $E'_\omega(0)$ have been taken to be real. From (8.90) we find

$$\frac{d|E'_{2\omega}|^2}{dz} = -\frac{d|E'_\omega|^2}{dz} \tag{8.92}$$

(in agreement with the Manley–Rowe relation), it is possible in this case to have 100% conversion of the input fundamental power into second-harmonic power.

As a first example of the solution of (8.90), we consider the case where there is an appreciable phase mismatch (by which we mean $l_{SH}\Delta k \gg 1$) so that little conversion of fundamental into SH is expected to occur. We therefore put $E'_\omega(z) = E'_\omega(0)$ on the right-hand side of (8.90a). The resulting equation can then be readily integrated [with the boundary condition $E'_{2\omega}(0) = 0$] to give

$$E'_{2\omega}(l) = -\frac{E'_\omega(0)}{l_{SH}}\left\{\frac{\exp(-i\Delta k l) - 1}{\Delta k}\right\} \tag{8.93}$$

from which we get

$$\left|\frac{E'_{2\omega}(l)}{E'_\omega(0)}\right|^2 = \frac{\sin^2(\Delta k l/2)}{(\Delta k l_{SH}/2)^2} \tag{8.94}$$

Since $|E'_{2\omega}|^2$ is proportional to the SH intensity $I_{2\omega}$, the variation of this intensity with crystal length is readily obtained from (8.94). According to (8.92), the behavior of I_ω must then be such that $I_\omega + I_{2\omega} = I_\omega(0)$. The dependence of $[I_{2\omega}/I_\omega(0)]$ and $[I_\omega/I_\omega(0)]$ on (l/l_{SH}) for $l_{SH}\Delta k = 10$ have both been plotted as dashed curves in Fig. 8.11. Note that, due to the large phase mismatch, only little conversion to second harmonic occurs. It can readily be shown from (8.94) that the first maximum of $[I_{2\omega}/I_\omega(0)]$ occurs at $l = l_c$, where l_c (the coherence length) is given by (8.49).

As a second example of the solution to (8.90), we consider the case of perfect phase matching ($\Delta k = 0$). In this case appreciable conversion to second harmonic may occur and the depletion of the fundamental beam must therefore be considered. This means that (8.90) must now be solved without the approximation that $E'_\omega(z) = E_\omega(0)$. If $\Delta k = 0$, however, it can be shown from (8.90) that $E'_{2\omega}$ and E'_ω are imaginary and real respectively. We can therefore write

$$E'_\omega = |E'_\omega| \tag{8.95a}$$

$$E'_{2\omega} = -i|E'_{2\omega}| \tag{8.95b}$$

and (8.90) then gives

$$\frac{d|E'_\omega|}{dz} = -\frac{1}{l_{SH}}\frac{|E'_{2\omega}||E'_\omega|}{E'_\omega(0)} \tag{8.96a}$$

$$\frac{d|E'_{2\omega}|}{dz} = \frac{1}{l_{SH}}\frac{|E'_\omega|^2}{E'_\omega(0)} \tag{8.96b}$$

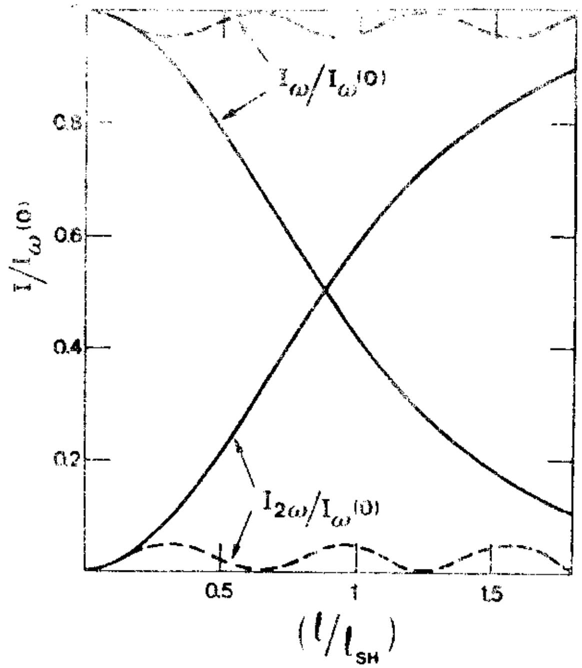

FIG. 8.11. Normalized plots of second-harmonic intensity $I_{2\omega}$ and fundamental intensity I_ω versus crystal length l for perfect phase-matching (continuous curves) and for a finite phase mismatch (dashed curves).

The solution of (8.96) with the boundary conditions $E'_\omega(l=0) = E'_\omega(0)$ and $E'_{2\omega}(0) = 0$ is

$$|E'_{2\omega}| = E'_\omega(0)\tanh(z/l_{SH}) \tag{8.97a}$$

$$|E'_\omega| = E'_\omega(0)\,\mathrm{sech}(z/l_{SH}) \tag{8.97b}$$

Since the intensity of the wave is proportional to $|E'|^2$, we have $I_{2\omega}/I_\omega(0) = |E'_{2\omega}|^2/E'^2_\omega(0)$ and $I_\omega/I_\omega(0) = |E'_\omega|^2/E'^2_\omega(0)$. The dependence of $I_{2\omega}/I_\omega(0)$ and $I_\omega/I_\omega(0)$ on crystal length as predicted by (8.97) is shown by the solid curves in Fig. 8.11. Note that, that for $l = l_{SH}$, an appreciable fraction (~59%) of the incident wave has been converted into SH. This illustrates the role of l_{SH} as a characteristic length for the second-harmonic interaction, with a value which is inversely proportional to the square root of the fundamental-beam intensity [see (8.91)]. Note also that for $l \gg l_{SH}$ the fundamental radiation can be completely converted into second-harmonic radiation, in agreement with the Manley–Rowe relation (8.92).

PROBLEMS

8.1. A Gaussian beam emitted by a visible He–Ne laser has a spot size (at the beam waist) of $w_0 = 0.5$ mm. Calculate the beam spot size and the radius of curvature of the equiphase surface at a distance of 10 m from the beam waist.

8.2. The Gaussian beam of the previous problem is to be focused to a beam waist of spot size 50 μm at a distance of 1 m from the original beam waist. What focal length should the lens have and where should the lens be placed?

8.3. A laser has a hemifocal resonator of length 50 cm. We want to place a lens after the spherical (output) mirror of the resonator to reduce the output beam divergence. If we require the spot size at the beam waist formed after the lens to be 0.95 times the beam spot size on the spherical mirror, what focal length must the lens have?

8.4. Prove equations (8.4).

8.5. Prove equation (8.10).

8.6. The output of a Q-switched Nd:YAG laser ($E = 100$ mJ, $\tau_p = 20$ ns) is to be amplified by a 6.3-mm-diameter Nd/YAG amplifier with a small signal gain $G_0 = 100$. Assuming a peak cross section of the laser transition of $\sigma \simeq 3.5 \times 10^{-19}$ cm^2, calculate the energy of the beam after the amplifier and hence the energy amplification. Also calculate the fraction of the stored energy in the amplifier which is extracted by the incident pulse.

8.7. A large Nd:glass amplifier to be used for fusion experiments uses a rod of 9 cm diameter and 15 cm length. The small signal gain of such an amplifier is 4. Taking the peak cross section of Nd:glass as $\sigma = 3 \times 10^{-20}$ cm^2, calculate the required input pulse energy (1-ns pulse) to generate an output of 450 J. What is the total energy stored in the amplifier?

8.8. A large CO_2 TEA amplifier (with a gas mixture CO_2:N_2:He in the proportion 3:1.4:1) has dimensions of $10 \times 10 \times 100$ cm. The small signal gain coefficient for the $P(20)$ transition is $g_0 = 4 \times 10^{-2}$ cm^{-1}. The duration of the input light pulse is 200 ns, which can therefore be taken to be much longer than the thermalization time of the rotational levels and much shorter than the decay time of the lower laser level. The peak cross section for the $P(20)$ transition under these conditions can be taken to be $\sigma = 1.54 \times 10^{-18}$ cm^2 and the partition function is $z = 0.07$ ($T = 300$°K). Calculate the output energy and gain available from this amplifier for an input energy of 17 J. Also calculate the energy per unit volume stored in the amplifier.

8.9. Prove that equation (8.39a) holds for a three-level system.

8.10. Prove equation (8.32).

8.11. Show that (8.56) gives $\sin^2\theta_m = [(n_2^o/n_1^o)^2 - 1]/[(n_2^e/n_1^o)^2 - 1]$, where n_2^o and n_2^e are the ordinary and extraordinary refractive indices at 2ω and where n_1^o is the ordinary refractive index at ω.

8.12. The frequency of a Nd:YAG laser output ($\lambda = 1.06$ μm) is to be doubled in a KDP crystal. Knowing that, for KDP, $n_o(\lambda = 1.06\ \mu\text{m}) \equiv n_1^o = 1.507$, $n_o(\lambda = 0.532\ \mu\text{m}) \equiv n_2^o = 1.5283$, and $n_e(\lambda = 0.532\ \mu\text{m}) \equiv n_2^e = 1.48222$, calculate the phase-matching angle θ_m.

8.13. Prove (8.69).

8.14. From (8.77) and (8.79) show that the threshold intensity of the pump wave for a DRO is $I = (n_3/2Zd^2)[n_1 n_2 \lambda_1 \lambda_2/(2\pi l)^2]\gamma_1\gamma_2$, where $Z = 1/\epsilon_0 c_0 = 377\ \Omega$ is the free-space impedance and λ_1 and λ_2 are the wavelengths of the signal and idler waves.

8.15. Using the result of the previous problem calculate the threshold pump intensity for parametric oscillation at $\lambda_1 \simeq \lambda_2 = 1$ μm in a 5-cm-long $LiNbO_3$ crystal pumped at $\lambda_3 \simeq 0.5$ μm [$n_1 = n_2 = 2.16$, $n_3 = 2.24$, $d \simeq 6 \times 10^{-12}$ m/V, $\gamma_1 = \gamma_2 = 2 \times 10^{-2}$]. If the beam is focused in the crystal to a spot of $\sim$100 μm diameter, calculate the resulting threshold pump power.

8.16. Calculate the second-harmonic conversion efficiency for type I harmonic generation in a perfectly phase-matched 2.5-cm-long KDP crystal with an incident beam at $\lambda = 1.06$ μm having an intensity of 100 MW/cm^2 [for KDP $n \simeq 1.5$, $d_{\text{eff}} = d_{36} \sin\theta_m = 0.28 \times 10^{-12}$ m/V, where $\theta_m \simeq 50°$ is the phase-matching angle].

REFERENCES

1. (a) N. Bloembergen, *Nonlinear Optics* (Benjamin, New York, 1965); (b) S. A. Akhmanov and R. V. Khokhlov, *Problems of Nonlinear Optics* (Gordon and Breach, New York, 1972).
2. O. Svelto, in *Progress in Optics*, Vol. XII, ed. by Emil Wolf (North-Holland, Amsterdam, 1974), pp. 3–50.
3. M. Born and E. Wolf, *Principles of Optics*, 4th ed. (Pergamon Press, London, 1970) Chapter X.
4. P. G. Kriukov and V. S. Letokhov, in *Laser Handbook*, ed. by F. T. Arecchi and E. O. Schulz-Dubois (North-Holland, Amsterdam, 1972), Vol. 1, pp. 561–595.
5. W. Koechner, *Solid-State Laser Engineering* (Springer-Verlag, New York, 1976), Chapter 4.
6. O. Judd, in *High-Power Gas Lasers*, ed. by E. R. Pike (The Institute of Physics, Bristol and London, 1976), pp. 45–57.
7. A. Yariv, *Introduction to Optical Electronics* (Holt, Rinehart and Winston, Inc., New York, 1971), Chapter 8.
8. S. A. Akhmanov *et al.* in *Quantum Electronics*, ed. by H. Rabin and C. L. Tang (Academic Press, New York, 1975), Vol. 1, Part B, pp. 476–583.
9. R. L. Byer, in *Quantum Electronics*, ed. by H. Rabin and C. L. Tang (Academic Press, New York, 1975), Vol. 1, Part B, pp. 588–694.
10. P. A. Franken *et al.*, *Phys. Rev. Lett.* **7**, 118 (1961).
11. J. A. Giordmaine and R. C. Miller, *Phys. Rev. Lett.* **14**, 973 (1965).
12. J. A. Giordmaine, *Phys. Rev. Lett.* **8**, 19 (1962).
13. P. D. Maker *et al.*, *Phys. Rev. Lett.* **8**, (1962).
14. F. Zernike and J. E. Midwinter, *Applied Nonlinear Optics* (John Wiley and Sons, New York, 1973), Section 3.7.
15. M. Lax, W. H. Louisell, and W. B. McKnight, *Phys. Rev. A* **11**, 1365 (1975).